

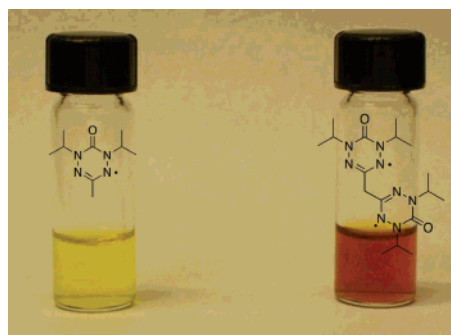
Radical–Radical Interaction through a Saturated Link: Methylenebis-6-oxoverdazyl

David J. R. Brook^{*,†} and Gordon T. Yee[‡]

Department of Chemistry, Santa Clara University, Santa Clara, California 95053, and Department of Chemistry, Virginia Polytechnic Institute and State University, Blacksburg, Virginia 24061

djbrook@scu.edu

Received January 24, 2006



The diradical methylenebis(1,5-diisopropyl-6-oxoverdazyl) was synthesized by benzoquinone oxidation of the corresponding bis(tetrazane). The diradical crystallizes in the monoclinic space group $C2/c$ with cell parameters $a = 21.1411(8) \text{ \AA}$, $b = 12.4781(5) \text{ \AA}$, $c = 8.2457(3) \text{ \AA}$, $\beta = 108.638(2)^\circ$, $V = 2061.15 \text{ \AA}^3$, $Z = 4$. Magnetic measurements indicate the diradical has a singlet ground state and triplet excited state at 150 cm^{-1} . Interaction between the nonconjugated radical centers is also seen in the UV–vis spectrum as a broad shoulder near 500 nm that is not apparent in the spectrum of the monoradical.

Introduction

Diradicals are objects of continuing fascination and study. In part, this arises from their importance in describing photochemical and thermal mechanistic pathways.^{1,2} More recently, diradicals and polyradicals have become model compounds for the understanding of molecular magnetism and the design of organic magnetic materials.³

Because of their unusual structure, diradicals frequently have one or more thermally accessible electronic excited states, in addition to the ground state. Though modern computational techniques and hardware can often calculate the multiplicities and energies of these states with reasonable accuracy, these calculations are still expensive, laborious, and not always reliable. Consequently, significant effort has been expended to develop readily applicable models to predict ground-state multiplicities and energies.^{4–6} Much work has focused on the

interactions of diradicals conjugated through π systems, using both matrix-trapped carbon radicals^{7–9} and more stable species such as nitroxides, nitronyl nitroxides,^{10–17} semiquinones,^{18–21}

[†] Santa Clara University.

[‡] Virginia Polytechnic Institute and State University.

(1) Klessinger, M.; Michl, J. *Excited States and Photochemistry of Organic Molecules*; VCH: New York, 1995.

(2) Borden, W. T. *Diradicals*; Wiley: New York, 1982.

(3) Lahti, P. M. *Molecular Magnetism in Organic-Based Materials*; Marcel Dekker: New York, 1999.

(4) Kahn, O. *Molecular Magnetism*; VCH: New York, 1993.

(5) Bonacic-Koutecky, V.; Koutecky, J.; Michl, J. *Angew. Chem., Int. Ed. Engl.* **1987**, *26*, 170–189.

(6) Salem, L.; Rowland, C. *Angew. Chem., Int. Ed. Engl.* **1972**, *11*, 92–111.

(7) Rajca, A.; Rajca, S. *J. Am. Chem. Soc.* **1996**, *118*, 8121–8126.

(8) Rajca, A.; Shiraishi, K.; Vale, M.; Han, H.; Rajca, S. *J. Am. Chem. Soc.* **2005**, *127*, 9014–9020.

(9) Luckhurst, G. R.; Pedulli, G. F.; Tiecco, M. *J. Chem. Soc. B* **1971**, 329.

(10) Fang, S.; Lee, M. S.; Hrovat, D. A.; Borden, W. T. *J. Am. Chem. Soc.* **1995**, *117*, 6727–6731.

(11) Fujita, J.; Tanaka, M.; Suemune, H.; Koga, N.; Matsuda, K.; Iwamura, H. *J. Am. Chem. Soc.* **1996**, *118*, 9347–9351.

(12) Oshio, H.; Makato, U.; Fukushi, T.; Ito, T. *Chem. Lett.* **1997**, 1065–1066.

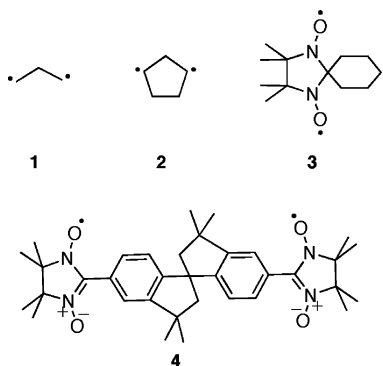
(13) Calder, A.; Forrester, A. R.; James, P. G.; Luckhurst, G. R. *J. Am. Chem. Soc.* **1969**, *91*, 3724–3727.

(14) Kawakami, T.; Yamanaka, S.; Mori, W.; Yamaguchi, K.; Kajiwara, A.; Kamachi, M. *Chem. Phys. Lett.* **1995**, *235*, 414–421.

(15) Kanno, F.; Inoue, K.; Koga, N.; Iwamura, H. *J. Am. Chem. Soc.* **1993**, *115*, 847–850.

(16) Wautelet, P.; Le Moigne, J.; Videva, V.; Turek, P. *J. Org. Chem.* **2003**, *68*, 8025–8036.

and verdazyls.²² Less well-investigated are coupling units involving tetrahedral carbons. This may be in part because of a perception that such coupling is weak. Without direct delocalization of the spin, interaction must be through dynamic spin polarization or hyperconjugation. Despite this, experimental and computational evidence supports significant magnetic interaction mediated by a single tetrahedral carbon. Several theoretical studies have focused on trimethylene (**1**) and shown that the triplet is more stable than the singlet as a result of a balance between through-space and through bond interactions.^{23–26} Experimentally, the diradical cyclopentane-1,3-diyl (**2**) has been shown to have a triplet ground state by Closs and co-workers.²⁷ Cyclopentane-1,3-diyls have proven to be a fruitful area of study; recent studies by Abe and co-workers have shown that the ground-state multiplicity can be manipulated by substituents on the bridging methylene group,²⁸ emphasizing the importance of the through bond interaction. In the realm of more stable systems, calculations suggest that nitroxides linked through CH₂ groups should show high-spin ground states (by $\sim 60\text{ cm}^{-1}$).²⁹ The dinitroxide **3** was synthesized by Keana and co-workers,³⁰ and though they demonstrated a large triplet zero-field splitting as a result of the close proximity of the free radicals, the multiplicity of the ground state was not determined. Shultz and co-workers investigated the interaction between three semiquinones linked by a single sp³ carbon and observed that the magnitude of the antiferromagnetic exchange was diminished by reduction of the third semiquinone to a catechol.^{31,32} Another study³³ investigated the electronic structure of a bisnitronyl nitroxide linked via two phenyl rings and a rigid sp³ carbon spacer (**4**). This molecule has a singlet ground state with a very small singlet–triplet separation (4 cm^{-1}).



Additional studies using stable free radicals may further understanding of through-bond vs through-space interactions.

(17) Stroh, C.; Zeissel, R.; Raudaschl-Sieber, G.; Kohler, F. H.; Turek, P. *J. Mater. Chem.* **2005**, *15*, 850–858.

(18) Cansechi, A.; Dei, A.; Lee, H.; Shultz, D. A.; Sorace, L. *Inorg. Chem.* **2001**, *40*, 408–411.

(19) Shultz, D. A.; Bodnar, S. H.; Lee, H.; Kampf, J. W.; Incarvito, C. D.; Rheingold, A. L. *J. Am. Chem. Soc.* **2002**, *124*, 10054–10061.

(20) Shultz, D. A.; Bodnar, S. H.; Kumar, R. K.; Lee, H.; Kampf, J. W. *Inorg. Chem.* **2001**, *40*, 546–549.

(21) Shultz, D. A.; Boal, A. K.; Farmer, G. T. *J. Am. Chem. Soc.* **1997**, *119*, 3846–3847.

(22) Fico Jr., R. M.; Hay, M. F.; Reese, S.; Hammond, S.; Lambert, E.; Fox, M. A. *J. Org. Chem.* **1999**, *64*, 9386–9392.

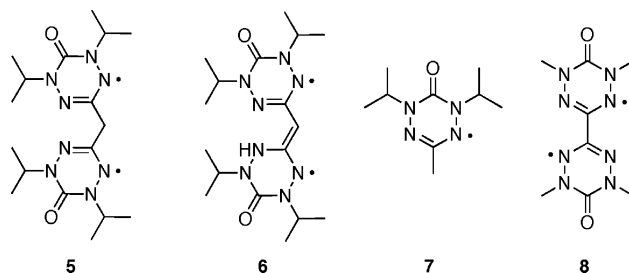
(23) Horsley, J. A.; Jean, Y.; Moser, C.; Salem, L.; Stevens, R. M.; Wright, J. S. *J. Am. Chem. Soc.* **1972**, *94*, 279–282.

(24) Goldberg, A. H.; Dougherty, D. A. *J. Am. Chem. Soc.* **1983**, *105*, 284–290.

(25) Doubleday, C., Jr.; McIver, J. W., Jr.; Page, M. *J. Am. Chem. Soc.* **1982**, *104*, 6533–6542.

(26) Hoffman, R. *Acc. Chem. Res.* **1971**, *4*, 1–9.

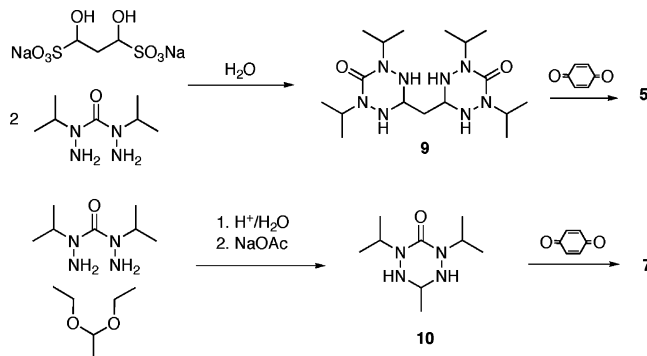
Methylene-linked verdazyls such as **5** may show additional unusual properties such as formation of tautomers (**6**) or deprotonation to form anions. Use of the recently reported *N*-isopropyl-substituted verdazyls³⁴ should ensure greater stability of these species in addition to supporting spectroscopy in a wide range of solvents. We report here the synthesis and characterization of the bis verdazyl **5** along with the monoradical analogue **7**. We also compare our results with the previously characterized 3,3'-bis(verdazyl) **8**.³⁵



Results

The diisopropylmethyl radical **7** and the methylenebis(verdazyl) **5** were synthesized using procedures developed previously.³⁴ These involved condensation of 2,4-diisopropyl-carbonohydrazide bishydrochloride with the corresponding aldehyde generated in situ from the bisulfite addition compound or the acetal (Scheme 1)

SCHEME 1. Synthesis of Verdazyls **5** and **7**



Oxidation with benzoquinone in toluene gave the verdazyl radicals, which are sufficiently volatile to be conveniently characterized by GC–MS. Monoradical **7** forms greenish-yellow crystals that can be readily purified by steam distillation. On standing in air at room temperature, **7** darkens slowly, presum-

(27) Buchwalter, S. L.; Closs, G. L. *J. Am. Chem. Soc.* **1979**, *101*, 4688–4694.

(28) Abe, M.; Adam, W.; Borden, W. T.; Hattori, M.; Hrovat, D. A.; Nojima, M.; Nozaki, K.; Wirz, J. *J. Am. Chem. Soc.* **2004**, *126*, 574–582.

(29) Okumura, M.; Takada, K.; Maki, J.; Noro, T.; Mori, W.; Yamaguchi, K. *Mol. Cryst. Liq. Cryst.* **1993**, *41*–60.

(30) Keana, J. F. W.; Norton, R. S.; Morello, M.; Van Engen, D.; Clardy, J. *J. Am. Chem. Soc.* **1978**, *100*, 934–937.

(31) Franzen, S.; Shultz, D. A. *J. Phys. Chem. A* **2003**, *107*, 4292–4299.

(32) Shultz, D. A. *J. Am. Chem. Soc.* **2001**, *123*, 6431–6432.

(33) Frank, N. L.; Clerac, R.; Sutter, J.-P.; Daro, N.; Kahn, O.; Coulon, C.; Green, M. T.; Golhen, S.; Ouahab, L. *J. Am. Chem. Soc.* **2000**, *122*, 2053–2061.

(34) Paré, E. C.; Brook, D. J. R.; Brieger, A.; Badik, M.; Schinke, M. *Org. Biomol. Chem.* **2005**, *3*, 4258–4261.

(35) Brook, D. J. R.; Fox, H. H.; Lynch, V.; Fox, M. A. *J. Phys. Chem.* **1996**, *100*, 2066.

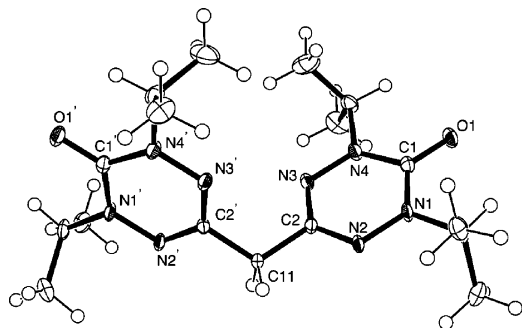


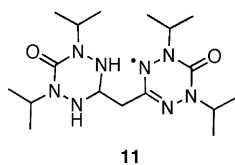
FIGURE 1. Thermal ellipsoid plot of **5**. The two verdazyl rings are related by a 2-fold axis passing through C11. Ellipsoids are plotted at the 50% probability level.

ably due to atmospheric oxidation. Diradical **5** is stable at room temperature in air and crystallizes as orange rhombi. Crystallographic analysis indicates that these have the monoclinic space group $C2/c$ with the molecule lying on a 2-fold axis passing through the central methylene carbon. A thermal ellipsoid plot is shown in Figure 1.

The verdazyl ring has bond lengths comparable to other 6-oxoverdazyls. The ring is almost planar; the two rings of one molecule are oriented 73° from each other. Each methylene C–H is 13.5° from the plane of one verdazyl ring but near perpendicular (76.3°) to the other. The C2–C11–C2' angle is 113.8° , and the C2–C2' distance is 2.52 \AA . The second closest distance between the two rings is 3.11 \AA between N3 and N3'. The isopropyl groups are oriented such that the C–H group is aligned with the C=O bond. The closest *intermolecular* ring–ring distance is 4.49 \AA between N2 of adjacent molecules.

The radical character of **5** and **7** was confirmed by ESR. In degassed toluene, **7** gives a well-resolved ESR spectrum with hyperfine coupling to all four nitrogen atoms, the isopropyl methine hydrogens, and the methyl hydrogens. Experimental and simulated spectra are shown in Figure 2.

In degassed *m*-xylene at room temperature, diradical **5** gives an ESR spectrum consisting of a signal showing significant hyperfine superimposed on a broad, featureless absorption. Simulation indicates that the broad line accounts for 99% of the signal; we thus assign this to the triplet state of **5**. The hyperfine can be simulated to give parameters consistent with a monoradical impurity **11** ($g = 2.0044$, $a_{N^{2,4}} = 6.48$, $a_{N^{1,5}} = 5.36$, $a_H = 1.55$ (2H), $a_{H'} = 1.59$ (2H)).



Upon freezing the solution, an ESR spectrum typical of a triplet is observed (Figure 3), with fine structure due to zero-field splitting in the $\Delta M_s = \pm 1$ region and a half-field signal ($\Delta M_s = \pm 2$) at 1680 G. A sharp signal remains at the center of the spectrum corresponding to the monoradical impurity previously mentioned; double integration confirms that this is a small proportion of the overall signal intensity ($\sim 1\%$).

Simulation of the $\Delta M_s = \pm 1$ region gave the zero-field splitting parameters $|D/hc| = 0.023 \text{ cm}^{-1}$ and $E \sim 0.0007 \text{ cm}^{-1}$. In organic systems, zero-field splitting is almost entirely due to the magnetic dipole–dipole interaction, which can be

estimated using the results of semiempirical calculations. Using the AM1 semiempirical Hamiltonian, a search for conformers of **5** about the central methylene carbon revealed the crystallographic geometry as the only energy minimum. Data from the AM1 calculation at the crystallographic geometry was used to estimate zero-field-splitting parameters³⁷ approximating the p orbitals as half charges 0.7 \AA above and below the plane of the verdazyl ring.^{9,35} This gave $|D|/hc = 0.025 \text{ cm}^{-1}$, $|E|/hc = 0.0004 \text{ cm}^{-1}$. Zero-field-splitting parameters were also estimated for the conjugated tautomer **6**. The structure was optimized at the AM1 semiempirical level, and the results were used to calculate $|D|/hc = 0.039 \text{ cm}^{-1}$, $|E|/hc = 0.007 \text{ cm}^{-1}$ using the same methods as above. The difference in magnitude of both parameters supports the assignment of the triplet spectrum to **5**. Examination of the temperature dependence of the signal intensity should give information as to the singlet–triplet splitting; however, over the accessible temperature range (140–200 K), the deviation from Curie behavior was small. Singlet–triplet splitting was consequently determined through magnetic susceptibility experiments.

Magnetic data were recorded on crystalline **5** between 5 and 300 K and corrected for sample diamagnetism using Pascal's constants. A plot of χT vs T is shown in Figure 4.

At room temperature, χT is slightly less than that for two uncorrelated spins. As the temperature is reduced, χT approaches a minimum near zero at 30 K and then increases slightly. Assuming that the low-temperature behavior is a result of the monoradical impurities that are visible in the ESR spectrum, the data can be fitted to a Bleaney–Bowers dimer model³⁸ with spin Hamiltonian $\hat{H} = -JS_1 \cdot S_2$, modified to account for a paramagnetic impurity. This model gives for χT (in emu K/mol)

$$\chi T = 3 \frac{(1-p)}{(3 + e^{J/k_b T})} + \frac{3}{8} p$$

where J is the singlet–triplet separation and p is the mole fraction of paramagnetic impurity. The best fit to this equation gives $J = -150(10) \text{ cm}^{-1}$ but also gives a negative value for p , which is not physically reasonable. The best-fit value of J is relatively independent of p ; estimation of the error in the fit gave an upper bound for p of 0.04 and with $p = 0.04$, J still minimizes to -150 cm^{-1} . A small positive value for p is consistent with the integration of the ESR spectrum. The possibility exists for *intramolecular* exchange, though we would expect this to be small based on the large intermolecular ring–ring distances. Consequently, the data strongly suggest that diradical **5** is a ground-state singlet.

Both **7** and **5** are soluble in hexane giving bright yellow and yellow-orange solutions, respectively. UV–vis spectra are shown in Figure 5.

For the monoradical **7**, two bands are clearly visible; the lower energy band shows distinct vibronic structure and is comparable to that reported for 1,3-dimethyl-6-oxoverdazyl.³⁹ The spectrum of **5** is very similar to that of **7** with two main bands, though the vibronic structure is less apparent. The molar absorptivity is approximately twice that of **7** which is consistent with two verdazyl chromophores. In addition, a lower energy band

(36) Duling, D. R. *J. Magn. Res. Ser. B* **1994**, *104*, 105–110.

(37) Prasad, B. L. V.; Radhakrishnan, T. P. *THEOCHEM* **1996**, *361*, 175–180.

(38) Bleaney, B.; Bowers, K. D. *Proc. R. Soc. London* **1952**, *A214*, 451.

(39) Neugebauer, F. A.; Fischer, H.; Siegel, R. *Chem. Ber.* **1988**, *121*, 815.

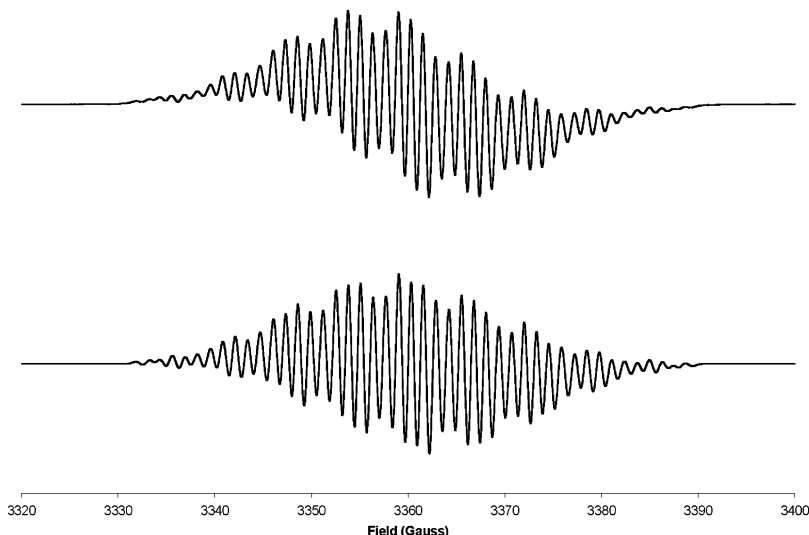


FIGURE 2. Experimental (top) and simulated (bottom) ESR spectra for **7**. The spectrum was recorded in degassed toluene. The program WINSIM³⁶ from the public EPR software tools (PEST) was used for simulation. Simulation parameters: $g = 2.0044$, $a_N^{1,5} = 5.27$ G, $a_N^{2,4} = 6.46$ G, $a_H(\text{Pr}) = 1.34$ G, $a_H(\text{CH}_3) = 2.35$ G, line width = 0.75 G.

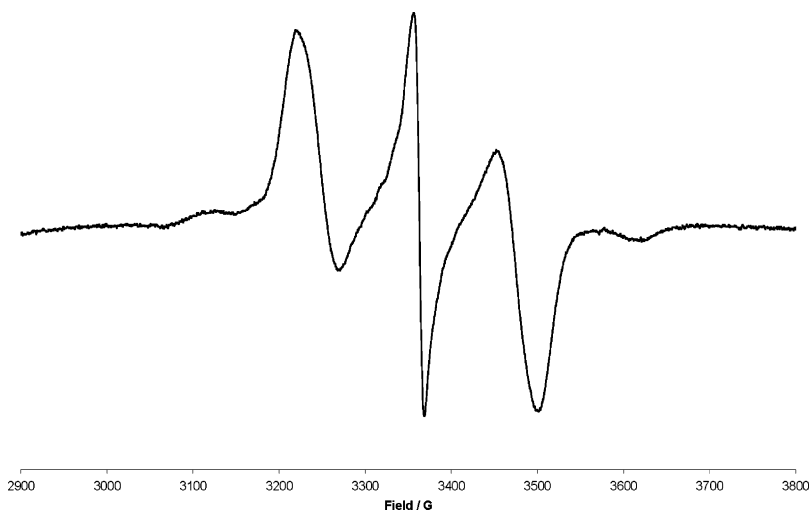


FIGURE 3. $\Delta M_s = \pm 1$ region of the ESR spectrum of **5** in frozen *m*-xylene at 165 K. The central sharp signal corresponds to the monoradical impurity **11**.

appears as a shoulder in the spectrum at 500 nm which accounts for the difference in color. The relative intensity of this band was essentially independent of temperature between 0 and 70 °C. The spectrum was also relatively solvent independent (solvents included ethanol, acetonitrile, toluene, and hexane) with the exception of an increase in resolution of the vibronic structure in hexane. A similar change in the resolution of the vibronic structure was observed for the monoradical **7**. Unless the energy difference between **5** and **6** is very small, this suggests that there is only one species in solution, most likely structure **5**. The equilibrium between singlet and triplet might also be expected to give temperature-dependent UV-vis spectra, though considering the magnitude of the singlet-triplet separation the effect would be small over the accessible temperature range. This combination of factors points to the additional band in the spectrum of **5** being due to a radical-radical interaction and not a conjugated tautomer.

Electrochemical measurements were performed on **5** and **7** in acetonitrile. Like other verdazyls, monoradical **7** undergoes reversible one-electron oxidation to the verdazylium ion and

one-electron reduction to the anion. These changes occur at potentials comparable to other 6-oxoverdazyls^{22,40} (0.6 V vs SCE for oxidation, -1.0 V for reduction). Diradical **5** is also reversibly oxidized. Cyclic voltammetry shows two close one-electron oxidation waves. These can be resolved by differential pulse voltammetry to give successive oxidations at 0.65 and 0.75 V vs SCE. The reduction of **5** is more complicated with a two-electron reduction at 1.0 V vs SCE. Similar behavior has been observed for other bis-verdazyls.²²

Despite numerous attempts with bases varying from NaOH to lithium hexamethyldisilazide, we were unable to characterize an anion corresponding to deprotonation of the central methylene group.

Discussion

A simple but useful model for a diradical system uses two delocalized molecular orbitals ϕ_1 and ϕ_2 , derived from sym-

(40) Barr, C. L.; Chase, P. A.; Hicks, R. G.; Lemaire, M. T.; Stevens, C. L. *J. Org. Chem.* **1999**, *64*, 8893.

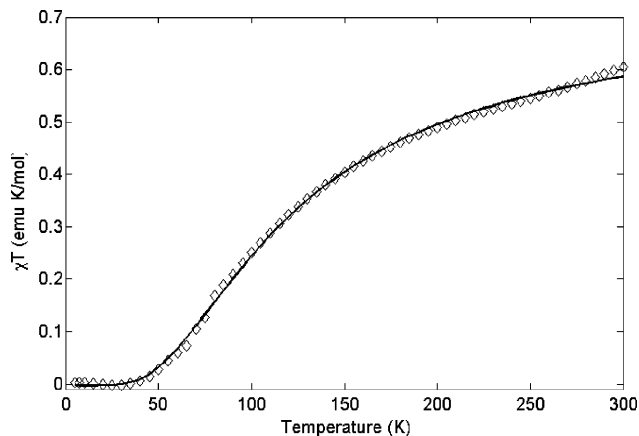


FIGURE 4. Plots of χT vs temperature for crystalline **5**. The solid line is a best fit to the Bleaney–Bowers dimer model described in the text with $J = -150 \text{ cm}^{-1}$, $p = 0$.

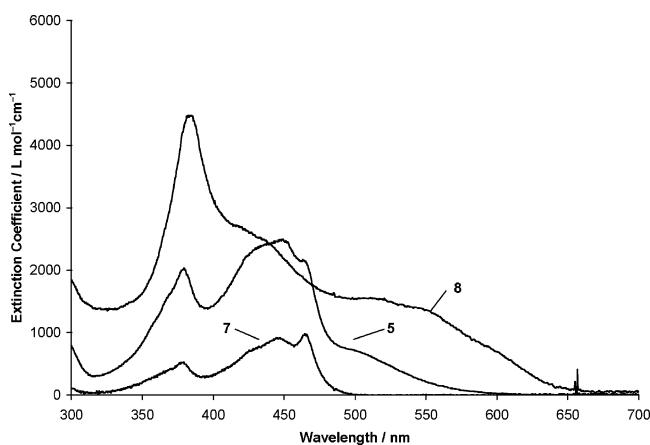


FIGURE 5. UV–vis spectra for monoradical **7** and diradical **5** in hexane. The spectrum of diradical **8** is also shown for comparison.

metric and antisymmetric combinations of the individual radical SOMOs. If these orbitals are degenerate, population with two electrons gives three singlets (S_0 , S_1 , S_2) and a triplet (T), the energies of which are controlled by the electron exchange integral K_{12} and the electronic repulsion term $K_{12}' = (J_{11} + J_{12})/2 - J_{12}$ where J_{11} , etc. is the usual Coulomb integral.^{1,5} The relative energies of the states are given by $E = E_0 \pm K_{12} \pm K_{12}'$. The lowest state is the triplet, while S_0 corresponds to a covalently bonded system and S_1 and S_2 correspond to charge-separated, ionic distributions of electrons. The nature of the S_1 and S_2 states is more apparent when a localized orbital basis is used.^{1,5}

Typically, however, the symmetric and antisymmetric combinations of SOMOs are not degenerate; interaction between the SOMOs allows one combination to become bonding, the other antibonding with an energy separation δ . This in turn has the effect of stabilizing the lowest singlet S_0 , and destabilizing the highest singlet S_2 . When $\delta > 2(K_{12}'(K_{12} + K_{12}'))^{1/2}$, S_0 drops below T; as δ increases further we start to approach something like a normal covalent bond.

While the S_0 –T separation is the value most commonly reported for diradicals, it only tells part of the story. At large radical–radical distances (and thus weak radical–radical interaction) both K_{12}' and δ will be small resulting in a small S_0 –T separation; alternatively, a small S_0 –T separation may

result from a fortuitous value of δ even though the radical centers interact relatively strongly. The S_0 – S_1 transition provides further information. Because the S_1 state has ionic character, the S_0 – S_1 transition corresponds to charge transfer between the radical centers. Accordingly, the intensity of the S_0 – S_1 transition is an indicator of overlap between SOMOs of the individual radical centers. The energy of the S_0 – S_1 transition corresponds to the sum of K_{12} (which approaches a maximum with increasing distance) and the S_0 –T separation.

In methylene-bridged radicals such as **5** there are two possible contributions to δ : through space and through bonds. Trimethylene provides the simplest example. In the 0–0 conformation (C_{2v} symmetry, with the two terminal p orbitals perpendicular to the C–C–C plane), interaction between the terminal radicals through space favors the symmetric combination of orbitals; hyperconjugative interaction through the CH_2 bond favors the antisymmetric combination. The effects are finely balanced, and the overall result is that δ is small while K_{12}' remains large and the triplet is slightly favored.^{24,26} The 1,3-cyclopentandiyl radicals first described by Closs provide a more extensively characterized example. In these systems, the same interactions are at play; the interactions through the ethylene bridge are minimal. The result is that the triplet ESR spectrum of **2** can be observed in rigid matrixes and appears to be the ground state. Ring closure, which is presumed to pass through the singlet state, requires an activation energy of 2.3 kcal/mol.²⁷ The role of the methylene bridge is highlighted by the recent reports of oxygen and fluorine substituted cyclopentane-1,3-diyls.²⁸ Substitution changes the interaction significantly enough to result in a singlet diradical ground state. These singlets show a strong absorption in the visible region assigned to the diradical S_0 – S_1 transition,²⁸ the energy of which correlates positively with the calculated singlet triplet splitting.

In verdazyl radicals, the unpaired electron is localized on the four nitrogen atoms; thus, in diradical **5** the most direct SOMO–SOMO interaction occurs between N3 and N3'. ESR of monoradicals **5** and **11** also indicates there is spin density on C2, presumably arising from dynamic spin polarization. As measured by hyperfine coupling to methyl hydrogens in monoradical **7** and *N*-methyl-substituted 6-oxoverdazyls,³⁹ spin density at C2 is approximately 45% of that at N1. This spin density provides a pathway for interaction through the methylene bridge, in addition to the direct C2–C2' interaction. Unfortunately, without further data we can do little more than speculate on the relative importance of these pathways; however, we can gain further insight into the radical–radical interaction by comparison of the UV–vis spectra with that of the isolated verdazyl. As noted previously, the UV spectrum of **5** is similar to that of **7** with the exception of a long wavelength shoulder near 500 nm. We assign this to the S_0 – S_1 transition of **5** by analogy with the cyclopentandiyls mentioned previously. This shoulder is the lowest energy feature in the spectrum. Transition to a higher energy triplet is also a possible assignment, but since such a state corresponds to population of higher energy verdazyl orbitals we expect the S_1 state to have the lower energy. Though the singlet–triplet separation is small, the observation of the S_0 – S_1 charge-transfer transition in the UV–vis indicates that the interaction between the verdazyl rings is significant.

The directly linked verdazyl diradical **8** also provides an interesting comparison. This diradical, initially reported in 1980⁴¹ and more fully characterized in 1996,³⁵ has also been the subject of a number of computational studies.^{42–44} Removal

of the methylene group from **5** decreases the separation of the verdazyl rings by ~ 0.7 Å. The unpaired electrons in **8** are closer together (as indicated by an increase in zero field splitting D from 0.023 cm^{-1} to 0.038 cm^{-1}) and experience greater mutual repulsion (as indicated by a greater difference between first and second $1e^-$ oxidation waves, 100 mV separation for **5** vs 250 mV for **8**). The closer approach of the rings does not, however, result in a large increase in bonding interactions, the S_0-T separation only increasing to 760 cm^{-1} . Inspection of Figure 5 reveals that **5** has a UV-vis spectrum intermediate between **7** (isolated radical) and **8**. The comparison suggests that the longest wavelength absorption of **8** should also be assigned to an S_0-S_1 transition. Interestingly, the relationship between S_0-T and S_0-S_1 is opposite of that observed for Abe's cyclopentanediyli systems. This is a result of the changes in CT energy resulting from the reduced radical separation dominating the effect of the increased singlet-triplet gap.

Conclusions

We have synthesized a methylene-bridged bisverdazyl with a singlet ground state and triplet excited state at 150 cm^{-1} . By analogy with cyclopentane-1,3-diyls, interradical interaction probably occurs both through space and through spin polarization of the intervening methylene group. ESR gives evidence for the latter, but resolution of the interaction into through-bond and through-space components is not possible with the available data. The UV-vis spectrum of the diradical shows a band due to the radical radical interaction and is intermediate between that of the monoradical and the directly linked diradical. We find no evidence for the existence of conjugated tautomers of **5** or for the deprotonation of the central methylene to give an anionic species.

Experimental Section

General experimental details are provided in the Supporting Information.

Di(1,5-diisopropyl-6-oxotetrazan-3-yl)methane (9). 2,4-Diisopropylcarbonohydrazide bishydrochloride (61 mg, 0.25 mmol) was combined with 37 mg (0.12 mmol) of malondialdehyde sodium bisulfite addition compound in 1 mL of water. To this solution was added an aqueous solution of sodium acetate (40 mg, 0.5 mmol) in 1 mL of water. The solution was allowed to stand for 15 h at room temperature during which time a white solid precipitated. Filtration gave di(1,5-diisopropyl-6-oxotetrazan-3-yl)methane (**7**) (36 mg, 76%): mp $134-140\text{ }^\circ\text{C}$ dec; $^1\text{H NMR}$ (CDCl_3) δ 4.57 (4H, septet, $J = 6.6\text{ Hz}$) 3.86 (2H, t, $J = 6.3\text{ Hz}$) 3.62 (bs, 4H), 1.74 (t, 2H, $J = 6.3\text{ Hz}$) 1.05 (d, 12 H, $J = 6.6\text{ Hz}$) 1.04 (d, 12 H, $J = 6.6\text{ Hz}$); $^{13}\text{C NMR}$ (CDCl_3) 154.4, 66.6, 47.1, 31.9, 19.4, 18.7, IR (NaCl plate) 3247 (NH), 2970, 2933 (CH), 1599 cm^{-1} (C=O); MS (EI, m/z) calcd for $\text{C}_{17}\text{H}_{36}\text{N}_8\text{O}_2$ 384, found 384 (2), 201 (50), 142 (55), 101 (100), 100 (45), 85 (38), 59 (55). GCMS (t_R 13.7 min) indicates the material is approximately 97% pure.

Methylene Bis(1,5-diisopropyl-6-oxoverdazyl) (5). Di(1,5-diisopropyl-6-oxotetrazan-3-yl)methane (27 mg, 0.07 mmol) was combined with benzoquinone (23 mg, 0.21 mmol) in 2 mL of toluene. The solution was heated under reflux for 5 h to give an orange-brown solution that precipitated hydroquinone on cooling.

(41) Neugebauer, F. A.; Fischer, H. *Angew. Chem., Int. Ed. Engl.* **1980**, *19*, 761.

(42) Barone, V.; Bencini, A.; Ciofini, I.; Daul, C. *J. Phys. Chem. A* **1999**, *103*, 4275-4282.

(43) Green, M. T.; McCormick, T. A. *Inorg. Chem.* **1999**, *38*, 3061-3065.

(44) Chung, G.; Lee, D. *Chem. Phys. Lett.* **2001**, *350*, 339-344.

The solution was filtered and evaporated to give an orange oil that was purified by chromatography on silica gel eluting with 5% v/v ethyl acetate in dichloromethane to give methylene bis(1,5-diisopropyl-6-oxoverdazyl) (**5**) as an orange crystalline solid (10 mg, 38%): mp $80-82\text{ }^\circ\text{C}$; IR (NaCl plate) 2978, 2935 (CH), $1676\text{ (C=O)}\text{ cm}^{-1}$; UV-vis (CH_3CN) 380 (2200), 440 (2600), 450 (2600), 500 (sh); MS (EI, m/z) calcd for $\text{C}_{17}\text{H}_{30}\text{N}_8\text{O}_2$ 378, found 378 (79), 336 (33), 294 (75), 252 (96), 210 (66), 181 (31), 139 (71), 138 (100). GCMS (t_R 11.56 min) indicates the material is approximately 99% pure.

Crystallography. Crystals of methylene bis(1,5-diisopropyl-6-oxoverdazyl), **5**, were obtained by slow evaporation of a heptane solution. The compound crystallized as orange irregular fragments, and a sample approximately $0.4 \times 0.3 \times 0.22\text{ mm}^3$ was used for data collection. Diffraction data were measured on a κ geometry CCD diffractometer with Mo radiation and a graphite monochromator at 100 K. Frames were collected as a series of sweeps with the detector at 40 mm for 3 s each and 0.3° between each frame. A total 1542 frames were collected, yielding 9059 reflections, of which 3442 were independent. The diradical crystallizes in the monoclinic space group $C2/c$ (No. 15) with unit cell dimensions $a = 21.1411(8)\text{ \AA}$, $b = 12.4781(5)\text{ \AA}$, $c = 8.2457(3)\text{ \AA}$, $\beta = 108.638(2)^\circ$, $V = 2061.15\text{ \AA}^3$, $Z = 4$. Solution and least-squares refinement gave $R(1) = 4.35\%$, $wR(2) = 12.05\%$. Full experimental crystallographic details are provided in the Supporting Information CIF format.

1,5-Diisopropyl-3-methyl-6-oxotetrazane (10). Acetaldehyde diethyl acetal (0.236 mg, 2 mmol) was combined with 1 drop of concd HCl and 0.5 mL of water. After the mixture stood at rt for 1.5 h, 2,4-diisopropylcarbonohydrazide bishydrochloride (0.5 g, 2 mmol) was added and the resulting mixture shaken to ensure complete solution. After a further 1 h, this was followed by a solution of sodium acetate (0.5 g) in 1 mL of water. An oily layer separated. The mixture was extracted with dichloromethane and the dichloromethane evaporated to give the crude tetrazane, recrystallized from ethanol/water to give a white crystalline solid (137 mg, 34%): mp $83-86\text{ }^\circ\text{C}$; $^1\text{H NMR}$ (CDCl_3) δ 0.99 (6H, d, $J = 6.6$), 1.01, (6H, d, $J = 6.6$), 1.21 (3H, d, $J = 5.6$), 3.41 (2H, br s, NH), 3.61 (1H, br q, $J = 5.6$), 4.53 (2H, septet, $J = 6.6$); $^{13}\text{C NMR}$ (CDCl_3) 16.46, 18.42, 19.32, 47.6, 65.65, 154.15; IR (film on NaCl plate) 3263 (NH), 3232 (NH), 2978 (CH), 2933 (CH), 1591 cm^{-1} (C=O); GCMS (t_R 7.7 min) indicates the material is approximately 98% pure with MS (EI, m/z) calcd for $\text{C}_9\text{H}_{20}\text{N}_4\text{O}$ 200, found 200 (30), 85 (100), 59 (28).

1,5-Diisopropyl-3-methyl-6-oxoverdazyl (7). A 100 mg sample of 1,5-diisopropyl-3-methyl-6-oxotetrazane (0.5 mmol) was combined with 81 mg (0.75 mmol) of benzoquinone in 2 mL of toluene and warmed on a hot plate. After a few minutes, black crystals of quinhydrone began to separate. Gentle heating was continued, and the black crystals were eventually replaced by white crystals of hydroquinone. After ~ 2 h, GC indicated that the reaction was complete. The solution was allowed to cool and the precipitated hydroquinone removed by filtration. Evaporation gave a yellowish-brown oil which was diluted with 10 mL of ethanol and 10 mL of water. Upon distillation of the solvent, the bright yellow free radical was carried over with the solvent vapor and collected in the receiver. Extraction of the collected distillate with dichloromethane and evaporation of the dichloromethane extract under a stream of nitrogen gave the free radical as a yellow oil that slowly crystallized on standing: IR (film, NaCl plate) 2965 (CH), 2877 (CH), 1682 cm^{-1} (C=O); GCMS (t_R 13.7 min) indicates the material is approximately 85% pure with MS (EI, m/z) calcd for $\text{C}_9\text{H}_{17}\text{N}_4\text{O}$ 197, found 197 (41), 182 (16), 155 (45), 113 (100), 99 (33), 83 (30), 70 (43), 56 (35).

Acknowledgment. D.J.R.B. thanks the Petroleum Research Fund (Grant No. 39923-B1) for partial support of this work.

G.T.Y. thanks the National Science Foundation for partial funding of the SQUID magnetometer. We also thank Dr. Mary-Jane Heeg for collection of the crystallographic data.

Supporting Information Available: General experimental details including ^1H NMR and ^{13}C NMR data for malondialdehyde

sodium bisulfite addition compound and Cartesian coordinates and calculated heat of formation for the optimized structure of **6**. Crystallographic data for **5** (CIF). This material is available free of charge via the Internet at <http://pubs.acs.org>.

JO060165B